Chaos, Solitons and Fractals 205 (2026) 117845

Contents lists available at ScienceDirect

Chaos, Solitons and Fractals

journal homepage: www.elsevier.com/locate/chaos

How subgroups affect the power law governing pedestrian avoidance interactions

Jingwei Ge [a], Wenhan Wu [b,*]

[a] University Research and Innovation Center, Obuda University, Budapest 1034, Hungary
[b] Senseable City Laboratory, Massachusetts Institute of Technology, Cambridge, MA 02139, USA

ARTICLE INFO

Keywords:
Pedestrian subgroups
Collision avoidance
Pedestrian interaction
Trajectory analysis
Nonlinear dynamics

ABSTRACT

Pedestrian motion, driven by continuous interactions that govern individual navigation and collective behavior, is crucial for understanding and managing complex crowd dynamics in urban public spaces. However, most existing studies treat pedestrians as isolated individuals, overlooking how subgroup organization affects collision avoidance and interaction laws. To address this, we develop a subgroup-aware framework to capture the most imminent subgroup-involved encounter by minimizing pairwise Time-To-Collision (TTC) within subgroups, thereby filtering redundant interactions and prioritizing behavioral realism. This data-driven analysis, applied to five public pedestrian datasets, examines the pair distribution function and interaction energy, showing that subgroup consideration yields a systematically smaller power-law exponent than the independent-individual assumption, revealing a weaker but more focused interaction decay. Moreover, the scaling exponent increases with subgroup size, indicating amplified repulsive forces and sharper avoidance maneuvers when facing larger subgroups. As an empirical feature-discovery study, these findings provide a more realistic and behaviorally grounded basis for modeling pedestrian dynamics, offering valuable implications for crowd simulation, public-space design, and autonomous systems.

1. Introduction

Pedestrian motion in public spaces is shaped by a continuous process of perceiving, anticipating, and responding to the movements of other individuals [1,2]. Whether on sidewalks, in transit stations, or across open plazas, these ubiquitous interactions determine not only how individuals navigate and move [3] but also how collective patterns such as lane formation [4], stripe formation [5], and stop-and-go waves [6] emerge. Therefore, understanding the mechanisms by which pedestrians adjust their trajectories in relation to neighbors is fundamental for explaining real-world movement behavior [7] and for developing reliable models of human movement [8]. These mechanisms lie at the core of a wide range of applications, including anomaly detection [9], crowd management [10], and autonomous navigation [11] in urban environments.

Nevertheless, translating empirical observations of pedestrian interactions into quantitative mathematical models inevitably requires simplifying assumptions. Most existing human motion models, whether data-driven laws [12] or force-based formulations [6,13], are implicitly built on the assumption that interactions occur between isolated individuals. In practice, however, a substantial fraction of pedestrians move as socially coordinated subgroups, such as friends, families, or colleagues, whose motion is goal-driven and exhibits shared intentions [14]. When subgroups are treated as independent individuals, interaction strength, perceived collision risk, and avoidance responses may be systematically misestimated. For instance, an oncoming pedestrian typically

* Corresponding author.
E-mail address: wenhanwu@mit.edu (W. Wu).

https://doi.org/10.1016/j.chaos.2025.117845
Received 19 November 2025; Received in revised form 22 December 2025; Accepted 27 December 2025

responds differently to a compact dyad than to two uncorrelated pedestrians, even if their spatial configuration appears similar [15]. Consequently, interaction laws summarized at the individual level [16] tend to fail to generalize to socially structured groups, limiting their descriptive power and predictive accuracy. To address this limitation, explicitly incorporating pedestrian subgroups into the quantification of avoidance behavior enables a more realistic characterization of pedestrian interactions, and provides empirical insights that can improve the calibration and validation of both data-driven and force-based models.

In this paper, we develop a subgroup-aware framework for characterizing pedestrian avoidance behavior in natural environments, positioned as an empirical data-analysis study focused on discovering key influences of subgroup-modulated dynamics. Specifically, pedestrian subgroups are first identified from public pedestrian datasets using a previously proposed network-based approach. Based on the identified results, an effective Time-To-Collision (TTC) metric is introduced for extending traditional pairwise interaction measurements, which can capture the most imminent encounter involving subgroups. Using this formulation, we systematically analyze the statistical properties of pedestrian interactions, including pair distribution function and interaction energy, revealing a remarkable difference in the scaling exponent when subgroups are taken into account. We further examine how subgroup size affects these interaction patterns, providing a hierarchical perspective that accommodates both isolated pedestrians and multi-member subgroups. This work integrates empirical data analysis with a generalized interaction law, aiming to advance the understanding of pedestrian dynamics in complex social contexts and to provide a foundation for more accurate crowd modeling. It should be emphasized that the interaction energy and the derived repulsive force are data-driven and statistical constructs that characterize the avoidance behavior of self-propelled pedestrians, rather than real physical energies or forces in the mechanical sense.

This paper is organized as follows. Section 2 reviews related work in this research field. Section 3 describes pedestrian trajectory datasets and subgroup identification results. In Section 4, the statistical quantification of pedestrian interactions is presented. Section 5 reveals the power law of subgroup-level interactions. Finally, the main conclusions, potential applications, and future directions are discussed in Section 6.

2. Related work

This section reviews the state of the art in pedestrian dynamics to contextualize our contributions. We first examine existing studies of pedestrian avoidance behavior, and then discuss a series of empirical findings regarding pedestrian subgroups. This synthesis highlights the critical gap in quantitative interaction models that explicitly account for social grouping, motivating the subgroup-aware framework proposed in this study.

2.1. Avoidance behavior in pedestrian interactions

A central question in the study of pedestrian behavior is how individuals avoid collisions with others when navigating shared spaces, and extensive efforts have been devoted to understanding the interaction mechanisms through various methods [17,18].

With regard to field observations, Karamouzas et al. [16] analyzed public pedestrian datasets and found that pedestrian interactions follow a universal power law governed by the anticipated TTC rather than spatial distance. Corbetta et al. [19] leveraged millions of real-life trajectories to study the avoidance interactions occurring in diluted conditions, constructing a Langevin-based model of binary avoidance in terms of both long-range (sight-based) and short-range (hard-contact avoidance) forces. In terms of controlled experiments, Murakami et al. [4] adopted a crowd experiment of lane formation and demonstrated how distracted pedestrians disrupt anticipatory interactions and delay the onset of collective pattern formation. In a subsequent experiment [20], these authors experimentally intervened pairs of pedestrians performing simple avoidance tasks and revealed that spontaneous coordination critically relies on mutual anticipation, rather than mutual gaze. Bacik et al. [21] combined theoretical analysis and controlled experiments to reveal that the order–disorder transition can be predicted by analyzing the geometry of pairwise interactions between pedestrians avoiding collision. For virtual reality (VR) technology, Kwon et al. [22] used an immersive VR road-crossing framework to examine the interactions between perceived crash risk and crossing behavior in a road with changes in environmental attributes. Liu et al. [23] utilized a VR platform to explore how pedestrians initiate detouring, select avoidance sides, and adjust lateral deviation when encountering a non-perceiving intruder.

2.2. Pedestrian subgroups in crowd dynamics

In recent years, an increasing number of studies have begun to recognize the pivotal role of pedestrian subgroups, owing to their ubiquity in real-world situations [24]. From the perspective of crowd dynamics, subgroups are typically defined as the set of pedestrians who move together with shared goals, social ties, and coordinated motion, and exhibit behavioral patterns that differ markedly from those of isolated individuals [14].

Empirical research has indicated several characteristic regularities associated with subgroups, such as subgroup size approximately following a (truncated) Poisson distribution [25], the decrease in average walking speed as subgroup size increases [24], and the transition of spatial configurations from horizontal to “V”-like or “U”-like structures as crowd density grows [26]. Turning to the avoidance behavior of mobile subgroups, such maneuvers can be interpreted as socially informed interactions with external individuals or subgroups. Bruneau et al. [27] conducted a VR-based user study to explore how real humans decide to go through or around subgroups, relevant results showed that the decision shift between these two choices is made according to some individual threshold. Gregorj et al. [28] utilized two pedestrian trajectory datasets to study the dynamics of collision avoidance between pedestrian subgroups (in particular dyads), confirming that the probability of passing through the subgroup is a decreasing function of interaction intensity and strength of social bonding. These authors [29] further investigated how dyads and singles navigate and avoid collisions in crowded environments, which revealed a systematic imbalance and significant effects of social interaction on avoidance behavior.

Table 1
Details of five public pedestrian datasets.

Dataset	Year	Location	No. ped	Flow type	Density range
Seq_eth	2009	Zurich, Switzerland	360	bidirectional	$0.007 \sim 0.181$ m^{-2}
Seq_hotel	2009	Zurich, Switzerland	389	bidirectional	$0.011 \sim 0.192$ m^{-2}
Crowds_zara01	2007	Nicosia, Cyprus	148	bidirectional	$0.012 \sim 0.239$ m^{-2}
Crowds_zara02	2007	Nicosia, Cyprus	204	bidirectional	$0.012 \sim 0.227$ m^{-2}
Students003	2007	Tel Aviv, Israel	434	multidirectional	$0.105 \sim 0.410$ m^{-2}

2.3. Research gaps

On the one hand, despite substantial progress in understanding pedestrian avoidance interactions at the individual level, existing research largely focuses on microscopic pairwise interactions or directly relates them to macroscopic collective patterns. From a mesoscopic perspective, the role of pedestrian subgroups as an intermediate organizational level remains insufficiently explored. This omission is nontrivial, as subgroups embody shared intentions, social bonds, and coordinated motion, which can fundamentally modulate how individuals perceive risk and execute avoidance maneuvers. On the other hand, while prior studies have documented characteristic properties of pedestrian subgroups, such as size distribution, walking speed, and spatial configuration, and have also examined their passing decisions or avoidance dynamics, a systematic quantification of avoidance interactions involving subgroups is still lacking. In particular, it remains unclear whether the governing principles identified for individual-level avoidance interactions can be extended to situations at the subgroup level, and how these principles are affected by subgroup size. As a result, filling this gap is essential for establishing a unified interaction framework that bridges individual-based avoidance laws and socially structured group motion, thereby providing a more realistic description of pedestrian dynamics in real-world environments.

3. Data preparation and subgroup identification

This section details the empirical data and processing pipeline that ground our statistical analysis. First, we introduce five public pedestrian datasets and describe the associated data preparation steps. Second, a previously proposed network-based algorithm is employed to identify pedestrian subgroups. These procedures provide the essential basis for our subsequent analysis.

3.1. Pedestrian trajectory extraction

This study utilizes the BIWI [30] and UCY datasets [31], chosen for their widespread use in pedestrian behavior research and for providing a representative variety of outdoor scenarios [32]. The BIWI dataset includes Seq_eth and Seq_hotel datasets, collected from a bird's-eye viewpoint at a frame rate of 2.5 FPS, capturing pedestrian movements near a university building and a bus station, respectively. The UCY dataset consists of Crowds_zara01, Crowds_zara02, and Students003 datasets, which were recorded at 25 FPS in open public spaces such as a shopping street and a university campus. Pedestrian trajectories in these sequences were manually or semi-automatically tracked and refined through post-processing to correct perspective distortion and reduce annotation errors. These datasets, summarized in Table 1, collectively provide a diverse representation of pedestrian motion patterns in natural outdoor environments, and differ in many aspects such as the number of pedestrians, density level, and flow type.

To ensure consistency across datasets and improve data quality, several preprocessing steps were applied to the extracted pedestrian trajectories. First, the trajectories from Seq_eth and Seq_hotel datasets, originally annotated at 2.5 FPS, were interpolated to achieve a unified frame rate of 25 FPS. This resampling ensured that the time interval between consecutive trajectory points can be standardized to 0.04 s, allowing for temporal consistency when combining all datasets and preventing potential biases caused by varying frame rates. Next, each trajectory was smoothed using a second-order low-pass Butterworth filter to suppress high-frequency noise and mitigate small oscillations due to tracking inaccuracies or frame-to-frame jitter. This filtering helps preserve the natural motion trends while eliminating fluctuations that do not reflect realistic pedestrian behavior. Finally, the instantaneous velocity of pedestrians was computed by a forward difference method based on consecutive position points. As shown in Fig. 1, the processed trajectories from all five datasets are visualized, serving as the data foundation for subsequent quantitative studies.

3.2. Pedestrian subgroup identification

In natural outdoor environments, pedestrians often move not as isolated individuals but as social subgroups, such as friends, families, or colleagues walking together. However, most previous studies merely focus on pairwise interactions between individuals and ignore the presence of subgroups that may significantly affect the underlying interaction laws. Therefore, we employ our previously proposed automatic method [33] to identify subgroups from video-based trajectory data. This approach integrates spatial proximity and temporal continuity to quantify the interaction intensity between pairs of pedestrians, where those who remain spatially close over a sustained period are assigned higher interaction intensities. From this, a time-dependent pedestrian flow network is constructed, with pedestrians represented as nodes and interaction intensities as weighted links. Potential subgroups are then identified as community structures in the network by applying an optimal threshold that maximizes the objective function of

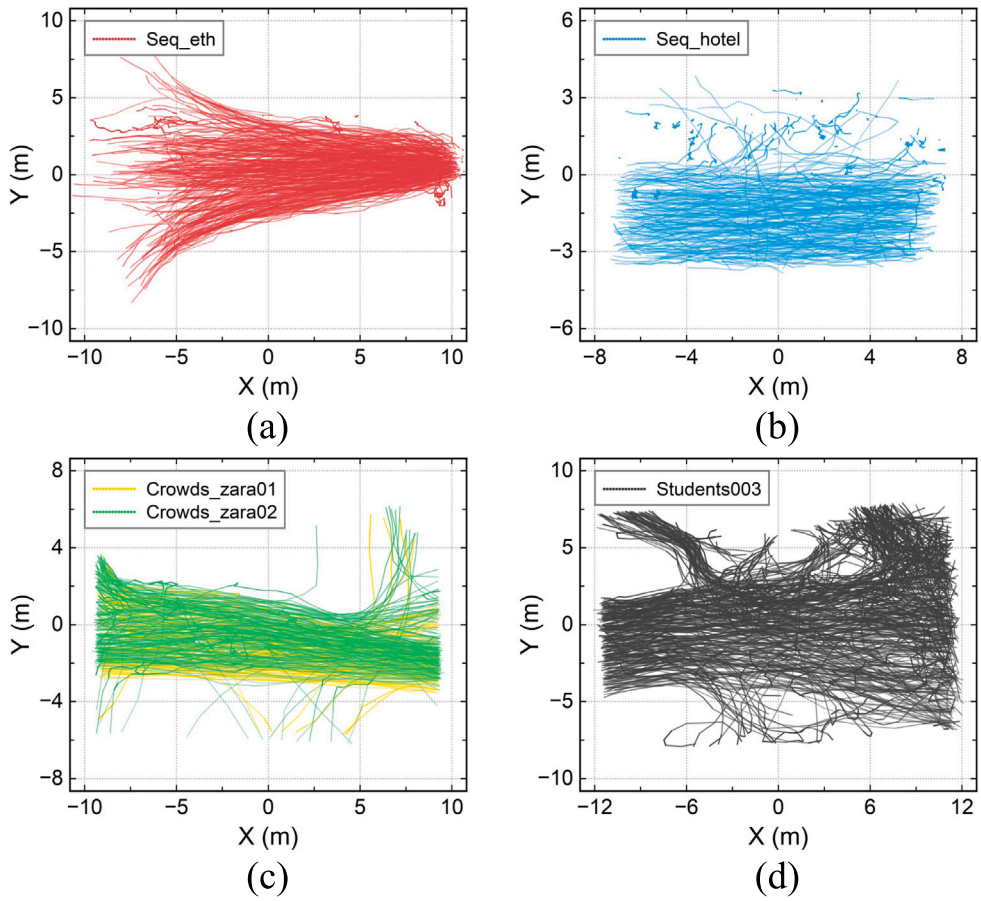

Fig. 1. Visualization of pedestrian trajectories in five public datasets. (a) Seq_eth. (b) Seq_hotel. (c) Crowds_zara01 and Crowds_zara02. (d) Students003. All trajectory coordinates in each scenario are translated to align the geometric center with the origin.

weighted partition density, which has been shown to achieve high identification accuracy on these five datasets [25,33]. To further improve accuracy, all automatically identified results were manually checked and calibrated to minimize detection errors.

To offer empirical support for the reliability of our detection results, Fig. 2 presents the quantitative characteristics of the identified pedestrian subgroups. Although slight variations exist across these five datasets due to differences in aspects such as scene configuration, crowd density, and social context, the proportion distribution typically decreases monotonically with increasing subgroup size in Fig. 2(a). Meanwhile, subgroups with more than four members are found to be extremely rare, which aligns well with previous empirical observations that subgroup sizes ranging from two to four are the most frequent in human crowds [25,26]. As a consequence, we focus on subgroups with sizes smaller than five. It can be observed from Fig. 2(b) that isolated individuals (note that they are treated as subgroups of size = 1) show higher average speeds compared to those walking in subgroups, whose average speeds tend to decrease as the size grows. This trend is consistent with the robust findings of subgroup walking speed [24], suggesting that larger subgroups move more slowly due to coordination and communication among members. Overall, these results demonstrate that the identified subgroups are reasonable and effective for our analysis of pedestrian interactions.

4. Statistical quantification of pedestrian interactions

In this section, we propose a modified TTC metric that specifically prioritizes the most imminent encounter involving subgroups, distinct from traditional pairwise interaction assumptions. Based on this metric, we derive two key statistical descriptors, pair distribution function and interaction energy, which allow us to quantitatively compare how the inclusion of subgroups alters the statistical quantification of pedestrian interactions.

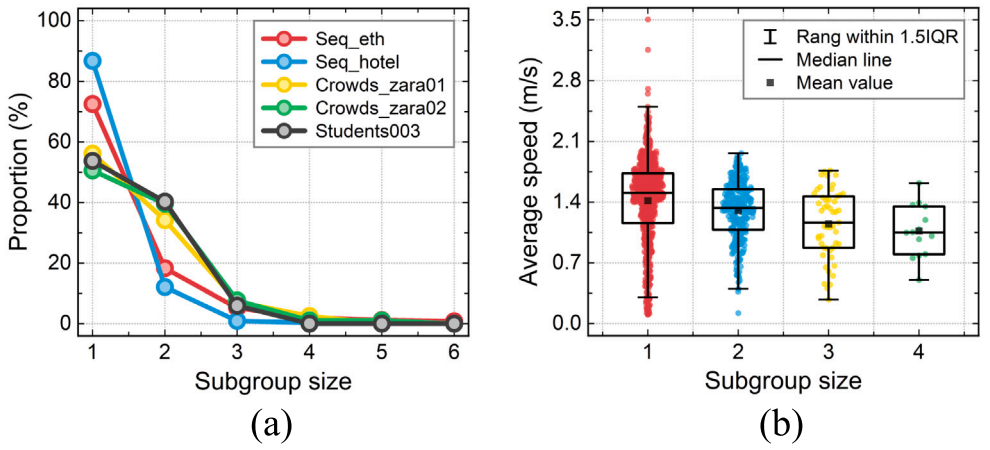

Fig. 2. Quantitative characteristics of the identified pedestrian subgroups. (a) Proportion distribution as a function of subgroup size. (b) Box plot of average speed for different subgroup sizes.

4.1. Time-to-collision

In this study, TTC is defined as the duration for which two pedestrians continue moving at their current velocities before colliding [6,16,34], which provides a dynamic measure of how imminent a potential collision is. A smaller TTC reflects a more imminent interaction context, indicating a stronger propensity for collision-avoidance behavior. This parameter inherently integrates both spatial and kinematic information, as it depends simultaneously on the relative position and velocity of two pedestrians. Specifically, the relative distance between pedestrians i and j at time t is $d_{ij}(t) = \left\|\vec{p}_i(t) - \vec{p}_j(t)\right\|$, where $\vec{p}_i(t)$ and $\vec{p}_j(t)$ are their positions. A potential collision is assumed to occur after a time period τ_{ij} if the relative distance $d_{ij}(t+\tau_{ij}) = \left\|\vec{p}_i(t+\tau_{ij}) - \vec{p}_j(t+\tau_{ij})\right\|$ equals the sum of their radii r_i and r_j (i.e., the two pedestrians touch each other). Note that the pedestrian radius is set to 0.1 m, following the same assumption as in Ref. [16]. The TTC τ_{ij} is found by solving the following equation:

$$\left\|\vec{p}_i\left(t+\tau_{ij}\right) - \vec{p}_j\left(t+\tau_{ij}\right)\right\| = r_i + r_j \tag{1}$$

where the new position of pedestrian i is calculated based on its current velocity $\vec{v}_i(t)$:

$$\vec{p}_i\left(t+\tau_{ij}\right) = \vec{p}_i(t) + \vec{v}_i(t)\cdot\tau_{ij} \tag{2}$$

Eq. (1) can be written as the quadratic equation:

$$A\tau_{ij}^2 + B\tau_{ij} + C = 0 \tag{3}$$

with parameters:

$$\begin{cases} A = \left\|\vec{v}_i(t) - \vec{v}_j(t)\right\|^2 \\ B = 2\left[\vec{v}_i(t) - \vec{v}_j(t)\right]\cdot\left[\vec{p}_i(t) - \vec{p}_j(t)\right] \\ C = \left\|\vec{p}_i(t) - \vec{p}_j(t)\right\|^2 - \left(r_i + r_j\right)^2 \end{cases} \tag{4}$$

Here, τ_{ij} is determined by the smallest positive root of the quadratic equation.

In the previous study, pedestrian interactions in human crowds were typically considered based on the hypothesis that each individual interacts independently with other individuals and neglects the presence of subgroups [16]. From this, this pairwise computational approach may produce multiple collision times when the encounter involves subgroups. Mathematically, let M and N be the nonempty sets of two subgroup members, the set of all admissible pairwise collision times between members $i \in M$ and $j \in N$ is defined as follows:

$$\mathcal{T}_{M,N}^{neg} = \left\{ \tau_{ij} \middle| i \in M, j \in N, \tau_{ij} < \infty \right\} \tag{5}$$

However, retaining all collision times in $\mathcal{T}_{M,N}^{neg}$ as independent interactions is not physically or behaviorally reasonable if subgroups are involved. In such cases, multiple members within a subgroup are sufficiently close in space and may generate highly correlated potential collisions with another pedestrian or subgroup. The corresponding motion state would change if one reacts to the most imminent collision, rendering the remaining predicted collisions invalid. From a cognitive insight, pedestrians also respond primarily to the most urgent threat, rather than processing all pairwise interactions simultaneously. The effective collision time $\tau_{M,N}^{con}$ considering subgroups is therefore defined as the minimum value of the set $\mathcal{T}_{M,N}^{neg}$:

$$\tau_{M,N}^{con} = \min\left(\mathcal{T}_{M,N}^{neg}\right) = \min\left\{ \tau_{ij} \middle| i \in M, j \in N, \tau_{ij} < \infty \right\} \tag{6}$$

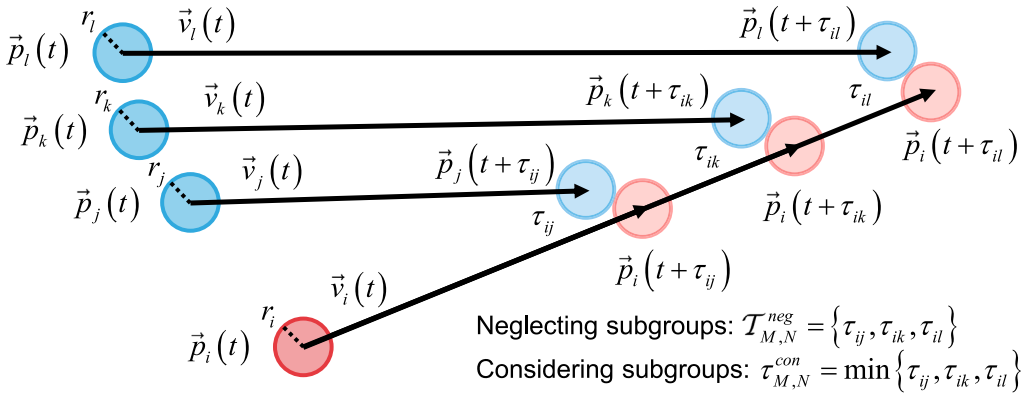

Fig. 3. Illustration of the encounter involving subgroups. A single pedestrian i (in red) interacts with a subgroup of members j, k, l (in blue). Each pairwise interaction yields a corresponding TTC if all pedestrians continue walking at their current velocities, denoted as τ_{ij}, τ_{ik}, and τ_{il}. (For interpretation of the references to color in this figure legend, the reader is referred to the web version of this article.)

This definition captures the earliest and thus most influential encounter, ensuring a more realistic representation of subgroup-related interactions. For further aspects of the above definitions see the example illustration in Fig. 3.

4.2. Pair distribution function

In condensed matter physics [35], the pair distribution function, $g(x)$, characterizes the degree to which different configurations are made unlikely by mutual interactions between particles. By analogy with pedestrian dynamics, this function is defined by:

$$g(x) = P(x)/P_{\mathrm{NI}}(x) \tag{7}$$

where $P(x)$ is the observed probability density of two interacting pedestrians at a relative separation x, and $P_{\mathrm{NI}}(x)$ is the expected probability density of two non-interacting pedestrians in an equivalent system. Given that non-interacting scenarios cannot be observed directly, the distribution $P_{\mathrm{NI}}(x)$ is approximated by constructing a time-scrambled dataset in which the time information in trajectory points is randomly permuted across individuals. This time-scrambled dataset keeps spatially-averaged density and time-averaged flow the same as in the original dataset, while ensuring that pedestrian positions at any given time are uncorrelated (i.e., pedestrians are not interacting).

Based on this, $g(\tau)$ as a function of TTC τ has been found to collapse onto each other across different approaching rates and relative orientations, which confirms that τ is a sufficient descriptor of pedestrian interactions. Notably, the magnitude of $g(\tau)$ reflects how pedestrian interactions influence the likelihood of pairwise configurations: $g(\tau) < 1$ indicates that configurations with a given collision time are suppressed due to avoidance behavior, while $g(\tau) > 1$ corresponds to configurations that are more likely than expected, often arising from coordinated or following motion, and $g(\tau) = 1$ represents an uncorrelated state where pedestrians move independently without systematic interaction effects. These classifications provide a systematic framework for characterizing the effects of pedestrian interactions on the structure of pairwise configurations. In the following analysis, we are particularly interested in examining how the incorporation of subgroups alters the statistical patterns of pedestrian interactions.

The pair distribution functions $g(\tau)$ obtained by neglecting and considering subgroup-level interactions are compared in Fig. 4(a). Both curves show a characteristic tendency: $g(\tau)$ increases sharply from near-zero at small interaction times ($\tau < 2$ s), indicating that imminent collision configurations are strongly suppressed due to mutual avoidance. In the intermediate range ($\tau = 2 \sim 4$ s), $g(\tau)$ gradually reaches a plateau, which reflects a stable interaction horizon where pedestrians continuously adjust their motion to maintain safe temporal margins. For long time scales $\tau > 4$ s, fluctuations around $g(\tau) = 1$ suggest that the interaction effect diminishes and pair configurations become statistically indistinguishable from random encounters. However, when subgroup-level interactions are considered, the statistical measure of $g(\tau)$ slightly decreases compared to the case of neglecting subgroups. This is because redundant pairwise interactions are filtered out, leaving only the most imminent encounters. This reduction does not imply weaker responsiveness but reflects organized and prioritized interactions with subgroup members, where individuals focus on the primary collision threat instead of responding to all potential interactions. Therefore, the difference between the two curves indicates that treating all pairwise links equally for subgroups tends to overestimate the apparent frequency of pairwise interactions.

4.3. Interaction energy

To gain a more physically interpretable description of the underlying interactions, it is critical to introduce the concept of energy to represent how strongly certain configurations are suppressed or favored. Assuming that the system is approximately in a statistical equilibrium state (i.e., macroscopic properties such as average pedestrian density and mean walking speed are almost time-invariant),

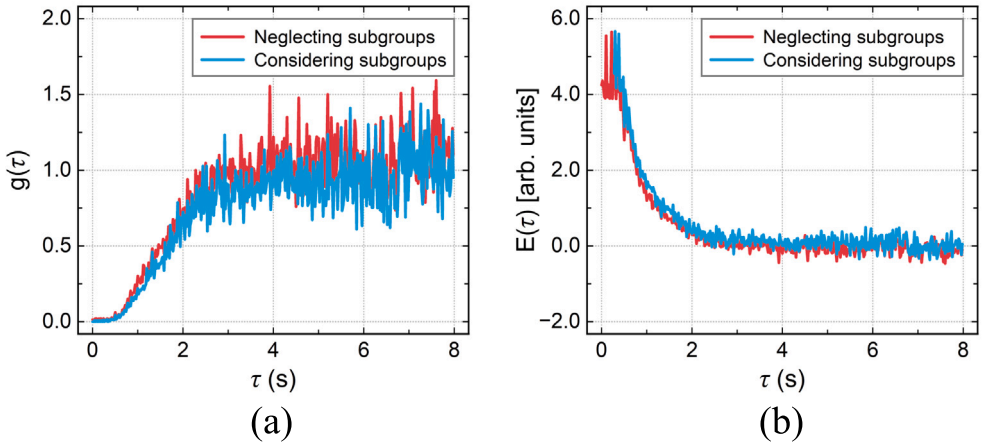

Fig. 4. Quantitative comparison of interaction statistics between the two cases of neglecting and considering subgroups. (a) Pair distribution function $g(\tau)$ as a function of TTC τ. (b) Interaction energy $E(\tau)$ as a function of TTC τ.

the pair distribution function $g(\tau)$ can be related to the interaction energy $E(\tau)$ through a Boltzmann-like relation. This facilitates the physical interpretation of avoidance behavior as a repulsive potential with a characteristic decay law, analogous to particle interactions in statistical mechanics, thereby quantifying how imminent collisions incur energetic costs due to mutual repulsion. Specifically, the probability of observing a pair of pedestrians with a given TTC τ is given by:

$$g(\tau) \propto \exp\left[-E(\tau)/E_0\right] \tag{8}$$

where E_0 is a characteristic energy scale depending on the scene conditions. This expression implies that configurations associated with stronger interactions (i.e., smaller τ) occur less frequently due to the effective repulsion between pedestrians. By rearranging this relation, the interaction energy can be expressed as follows:

$$E(\tau) \propto \ln\left[1/g(\tau)\right] \tag{9}$$

From this, the interaction energy $E(\tau)$ provides a quantitative measure of how interaction strength varies with the imminence of collision.

Fig. 4(b) illustrates how the interaction energy $E(\tau)$ varies with the TTC τ. Regardless of whether subgroups are considered, $E(\tau)$ exhibits a consistent pattern: it starts from large values at small τ, decreases rapidly with increasing τ, eventually approaches zero and remains relatively stable at large τ. This tendency indicates that configurations with small τ (i.e., imminent collisions) are statistically suppressed, as pedestrians actively avoid such situations, thereby leading to high energetic costs. In contrast, configurations with large τ (i.e., distant or non-interacting pairs) occur more frequently than expected, reflecting low interaction energy states where mutual influence is negligible and pedestrian motion is largely independent. Interestingly, when subgroups are taken into account, the overall trend of $E(\tau)$ remains almost consistent but the curve shifts slightly upward. This enhancement arises naturally from the inverse relation between $E(\tau)$ and $g(\tau)$, but it also carries a clear physical interpretation. By eliminating redundant pairwise links, subgroup-level interactions effectively concentrate efforts on the most relevant encounters, resulting in less but stronger interaction responses. In energetic terms, this means a higher interaction strength toward imminent threats, which translates into elevated $E(\tau)$ despite an overall reduction in interaction frequency. As a result, this reveals a more selective but energetically focused interaction strategy with respect to subgroups.

5. Power law of subgroup-level interactions

This section presents the core empirical analysis of the power law of pedestrian interactions. We first compare how the interaction energy decays with TTC in a power-law form under individual-based versus subgroup-based assumptions, and then examine how subgroup size influences the decay exponent and overall interaction law.

5.1. Power-law fit of interaction energy

In this part, we are interested in exploring the interaction law of pedestrian motion. The visual inspection of interaction energy curves in Fig. 4(b) reflects a systematic decay pattern: $E(\tau)$ attains large values at very small τ (plausibly due to finite human reaction limits), then falls off significantly over an intermediate range, and finally levels off near zero at large τ (interaction truncation caused by excessive collision times). This suggests that $E(\tau)$ is only well defined over a finite interval of τ, within which the measured energy varies smoothly from the region of large-range fluctuations to the region where it becomes indistinguishable from noise. To

determine this valid interval, we adopt the quantitative clustering to divide the values of τ into uniform intervals (bins of 0.2 s). The lower boundary is defined as the point $\tau_{\min}$ where the interaction energy first shows a significant decline between successive bins (we use t-test here), reflecting the onset of actual interaction effects beyond strong energy fluctuations. The upper boundary is determined as the point $\tau_{\max}$ where $E(\tau)$ approaches a steady level and exhibits no noticeable variation across successive bins (we use ANOVA test here), indicating that interactions at longer timescales contribute negligibly to the measured energy.

Within the identified interval $\left[\tau_{\min}, \tau_{\max}\right]$, the interaction energy $E(\tau)$ exhibits a monotonic decay, implying a potential scaling relation. To quantitatively capture this scaling law, we perform a power-law fit of interaction energy as follows:

$$E(\tau) \propto \tau^{-\alpha} \tag{10}$$

where α quantifies the rate of decay for interaction energy. The fitting is carried out in logarithmic space using a least-squares regression on $\log E(\tau)$ versus $\log \tau$, which linearizes the relationship and allows for a robust estimation of the exponent. To mitigate the influence of statistical outliers and local fluctuations, the bisquare weighting is applied to ensure that the power-law fit reflects the central trend of the observed data. The above procedures give a complete derivation process of the interaction law, which will be compared across different conditions in the following subsections.

5.2. Effect of subgroup consideration on interaction law

We now compare the interaction law under two conditions: neglecting and considering pedestrian subgroups. The first case corresponds to the previous study [16], where all pedestrians are treated as independent individuals, each assumed to interact pairwise with others regardless of any subgroup affiliation. The second case explicitly incorporates subgroup-level interactions, in which the effective interaction is governed by the earliest (most imminent) collision with subgroup members. Following the approach described in the previous subsection, the well-defined interval $\left[\tau_{\min}, \tau_{\max}\right]$ is determined separately for each case. For the case of neglecting subgroups, the lower boundary is $\tau_{\min} = 0.6$ s [$t(18) = 4.574$, $P < 0.001$], and the upper boundary is $\tau_{\max} = 2.6$ s [$F(2, 27) = 1.741$, $P = 0.194$]. For the case of considering subgroups, we have the lower boundary $\tau_{\min} = 0.6$ s [$t(18) = 5.003$, $P < 0.001$] and the upper boundary $\tau_{\max} = 2.4$ s [$F(2, 27) = 0.305$, $P = 0.740$]. In both cases, as shown in Fig. 5(a)–(b), $E(\tau)$ varies smoothly within the identified interval $\left[\tau_{\min}, \tau_{\max}\right]$, without the strong initial fluctuations or the nearly constant tail observed in the raw data. This determines a reliable region over which the interaction energy remains physically meaningful for scaling analysis.

Here, the interaction energy $E(\tau)$ is examined in logarithmic space, we conduct a linear fit with bisquare weighting to quantify the scaling law. The log–log plots in Fig. 5(c)–(d) reveal that $E(\tau)$ follows a power-law decay with increasing τ over the well-defined interval, which confirms the same scale-invariant nature of pedestrian interactions under both assumptions. Notably, the exponent α differs between these two cases: $\alpha = 1.932 \pm 0.083$ for the case when subgroups are neglected, aligning well with the previous finding that E shows a quadratic falloff as a function of τ. However, the case of considering subgroups yields a smaller exponent of $\alpha = 1.693 \pm 0.105$, indicating a slower decay of interaction energy. The difference arises because retaining only the most imminent interaction weakens the short time-scale concentration of energy, resulting in a more gradual overall decay and thus a smaller power-law exponent. This highlights that subgroup-related interactions reflect a less rapidly dissipating energy response pattern compared to treating all individuals independently.

5.3. Effect of subgroup size on interaction law

For the case of considering subgroups, the influence of subgroup size on the power law governing pedestrian interactions is further investigated. We focus on isolated individuals and the most frequently observed subgroup sizes (i.e., dyads, triads, and tetrads) in human crowds, and define the interactions associated with subgroup size N_s as those between a subgroup of size N_s and another subgroup with size $\leq N_s$. This definition ensures that the effective interaction for subgroup size N_s is evaluated with respect to all relevant encounter partners, thereby preserving a consistent hierarchical structure in the scope of interactions across subgroup sizes. Following the same procedures as before, the linear fit of interaction energy $E(\tau)$ for each subgroup size is performed over the well-defined interval. Fig. 6 denotes that all four cases consistently follow a power-law decay regardless of subgroup size. This demonstrates that the scale-invariant structure of pedestrian interactions remains robust even when subgroup heterogeneity is taken into account.

In particular, the fitted power-law exponent α increases systematically with subgroup size: isolated individuals ($N_s = 1$) exhibit the smallest exponent, whereas dyads ($N_s = 2$), triads ($N_s = 3$), and tetrads ($N_s = 4$) show progressively larger exponents. This tendency reflects that interactions involving larger subgroups display a steeper decay of $E(\tau)$ with increasing τ. A plausible explanation stems from the definition of avoidance-based interaction. Pedestrians typically experience a greater sense of pressure when encountering larger subgroups, which amplifies their short-time collision sensitivity and increases the energetic cost of evasive maneuvers. In other words, larger subgroup contexts will intensify immediate avoidance effort, producing the observed increase in the fitted exponent. As a consequence, the exponent α reflects how subgroup size shapes the scaling behavior of pedestrian interactions, highlighting the critical role of subgroup organization in governing the emergent interaction law in human crowds.

Although subgroup size primarily modifies the short-time scaling through changes in the exponent α, the decay of interactions at larger τ is governed by a characteristic cutoff τ_0 that reflects the limited anticipation range of pedestrians. The cutoff times across all subgroup conditions consistently cluster around the observed value $\tau_0 \approx 3$ s (in line with the previous report indicating a $2 \sim 4$ s time window [36]), allowing us to identify a lower bound estimate of the intrinsic interaction horizon. Therefore, the final

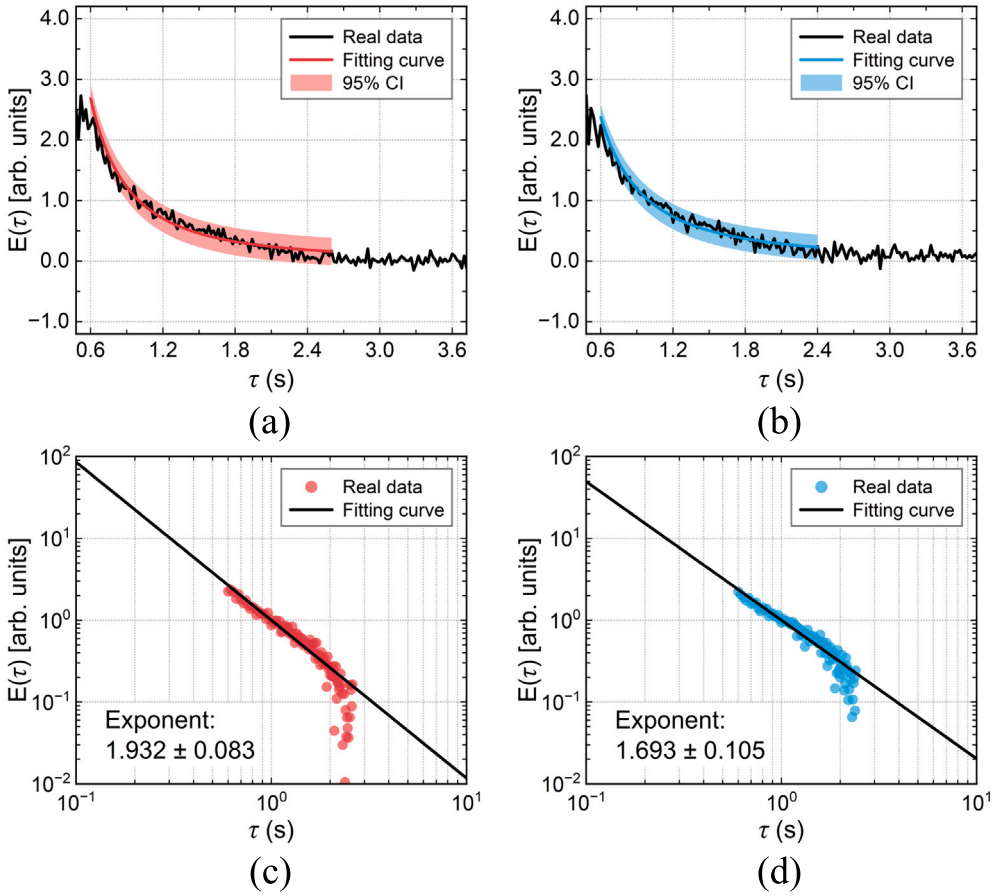

Fig. 5. Comparison of the power law of pedestrian interactions under different assumptions. (a)–(b) Interaction energy $E(\tau)$ as a function of TTC τ for the two cases of neglecting and considering subgroups. The solid line and colored region represent the fitting curve and 95% confidence interval, respectively. (c)–(d) Power-law relationship between interaction energy $E(\tau)$ and TTC τ for the two cases of neglecting and considering subgroups. The colored circles and solid line denote the real data and fitting curve in logarithmic space, respectively. Note that the data are normalized so that $E(1) = 1$.

mathematical form of the interaction energy exhibits a power-law dependence for short avoidance times with a sharp truncation beyond the interaction horizon:

$$E(\tau) = \frac{k}{\tau^{\alpha}} \exp\left(-\tau/\tau_0\right) \tag{11}$$

Here, the constant k sets the units for energy. With the energy function specified, its gradient directly $-\nabla_{\vec{p}_{ij}} E(\tau)$ yields the interaction force acting on pedestrians:

$$\vec{F}_{ij} = -\left[\frac{k e^{-\tau/\tau_0}}{\left\|\vec{v}_{ij}\right\|^2 \tau^{\alpha}}\left(\frac{\alpha}{\tau} + \frac{1}{\tau_0}\right)\right]\left[\vec{v}_{ij} - \frac{\left\|\vec{v}_{ij}\right\|^2 \vec{p}_{ij} - \left(\vec{p}_{ij}\cdot\vec{v}_{ij}\right)\vec{v}_{ij}}{\sqrt{\left(\vec{p}_{ij}\cdot\vec{v}_{ij}\right)^2 - \left\|\vec{v}_{ij}\right\|^2\left(\left\|\vec{p}_{ij}\right\|^2 - \left(r_i + r_j\right)^2\right)}}\right] \tag{12}$$

It can be seen from Fig. 7(a)–(b) that higher interaction energy associated with larger subgroups naturally leads to stronger psychological repulsive forces during encounters. Such amplified forces manifest as sharper turns and more abrupt avoidance, which is consistent with empirical observations that pedestrians react more vigorously to larger oncoming groups due to increased collision risk and spatial pressure [28].

6. Conclusions

In this work, we revisit the fundamental interaction law governing pedestrian motion by explicitly incorporating the role of subgroups in human crowds. Using trajectory data in five public pedestrian datasets, pedestrian subgroups are identified through

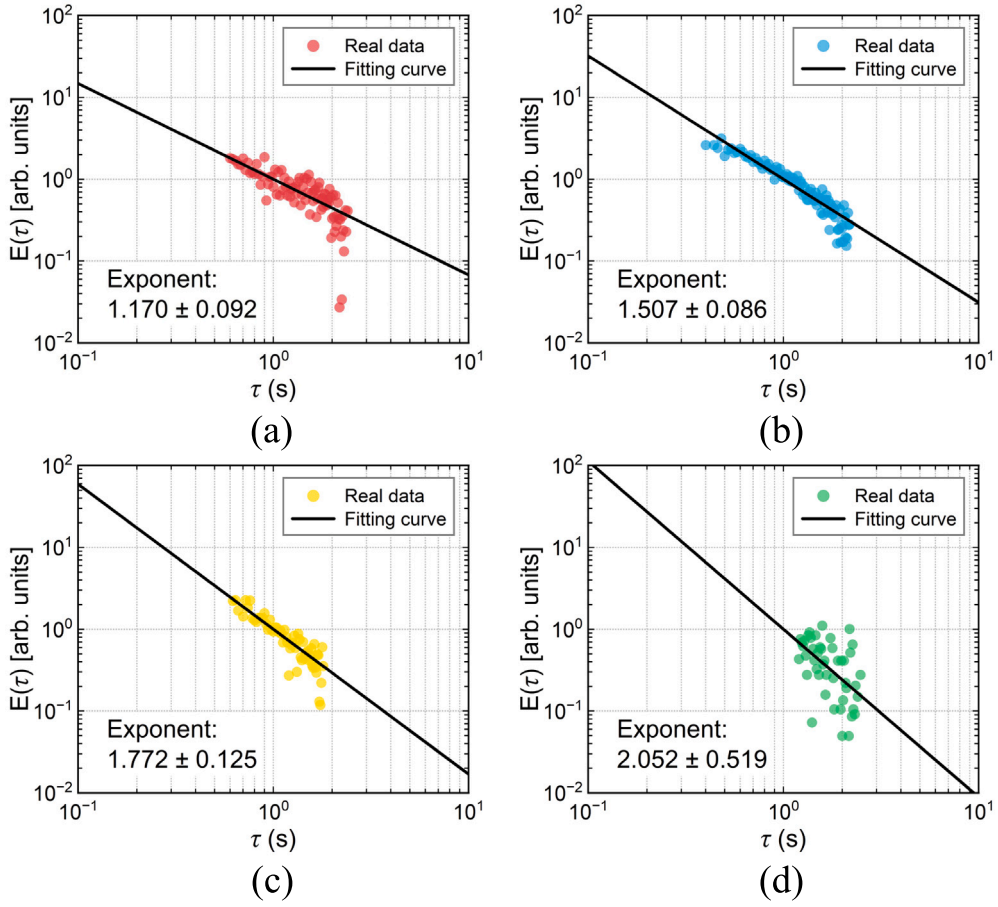

Fig. 6. Comparison of the power law of pedestrian interactions under different subgroup sizes. (a) Subgroup size = 1. (b) Subgroup size = 2. (c) Subgroup size = 3. (d) Subgroup size = 4. The colored circles and solid line denote the real data and fitting curve in logarithmic space, respectively. Note that the data are normalized so that $E(1) = 1$.

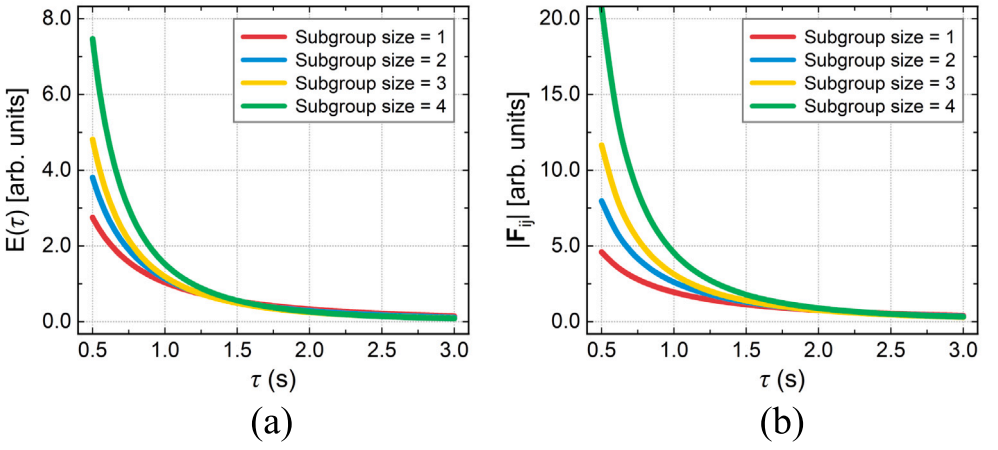

Fig. 7. Interaction energy and force for different subgroup sizes. (a) Interaction energy $E(\tau)$ as a function of TTC τ. (b) Interaction force $|\vec{F}_{ij}|$ as a function of TTC τ. The scalar is derived under the simplifying assumption that $\vec{p}_{ij}$ and $\vec{v}_{ij}$ are collinear and oppositely directed, with the initial separation normalized to unit distance.

a previously proposed network-based method. Building on this, we improve the classic pairwise interaction framework by defining an effective TTC that reflects the most imminent encounter involving subgroups. This subgroup-aware formulation enables a reassessment of the pair distribution function and the associated interaction energy. Our results show that although the overall trend of pedestrian interactions remains robust, considering subgroups reduces redundant pairwise links and yields a more selective and energetically focused interaction pattern. The interaction energy retains a clear power-law decay, but with a smaller exponent compared to the case of neglecting subgroups. Moreover, the increasing scaling exponent for larger subgroups amplifies the effective repulsive force, which may lead to sharper turning maneuvers and stronger avoidance actions during imminent encounters.

These findings link subgroup structure directly to measurable changes in the pedestrian interaction law, particularly the modified scaling exponent and the size-dependent repulsive interactions. This provides a behaviorally grounded basis for microscopic crowd simulation models [37], where explicitly accounting for the presence and size of subgroups helps avoid inaccurate estimation of interaction strength and better captures sharp avoidance maneuvers during imminent encounters. It can also inform the design and safety evaluation of pedestrian-oriented public spaces (e.g., transport hubs, urban walkways, and large-scale event venues) [38], because the effects of subgroups on interaction behavior and pedestrian flow can be quantified, which enables more realistic predictions and targeted interventions to reduce congestion and enhance safety. In addition, the refined interaction descriptors support downstream tasks (e.g., trajectory forecasting, human–robot navigation, and autonomous-vehicle planning) in computer vision and robotics [39,40], where anticipating subgroup-driven coordinated motion is very critical for safe and socially compliant decision-making.

Despite these advances, several limitations should be indicated as well. First, the subgroup identification relies on trajectory-based cues rather than richer multimodal information such as gaze direction or social context [41], which may overlook subtle coordination and avoidance behaviors in complex social settings. Second, the analysis focuses on encounters between pairs of entities, whereas higher-order interactions [42] in human crowds may involve more intricate decision-makings and movement behaviors. Third, while the interaction energy provides a physically interpretable description of pedestrian avoidance, it does not correspond to actual physical mechanisms between self-propelled pedestrians, who act based on perception and anticipatory decisions. Nevertheless, our framework demonstrates that acknowledging subgroup structure is essential for uncovering the true power law of pedestrian interactions. Future work may incorporate additional behavioral signals for more robust subgroup detection, extend the interaction law to multi-party encounters, and explore how environmental and cultural factors affect the interaction behavior. In conclusion, these directions offer a pathway toward a more comprehensive theory of pedestrian interactions.

CRediT authorship contribution statement

Jingwei Ge: Writing – original draft, Validation, Software, Resources, Methodology, Formal analysis, Data curation, Investigation, Writing – review & editing. **Wenhan Wu:** Writing – original draft, Visualization, Validation, Supervision, Methodology, Data curation, Conceptualization, Software, Formal analysis, Writing – review & editing.

Declaration of competing interest

The authors declare that they have no known competing financial interests or personal relationships that could have appeared to influence the work reported in this paper.

Data availability

Data will be made available on request.

References

[1] Fan Z, Loo BP. Street life and pedestrian activities in smart cities: opportunities and challenges for computational urban science. Comput Urban Sci 2021;1(1). http://dx.doi.org/10.1007/s43762-021-00024-9.
[2] Elzeni MM, ELMokadem AA, Badawy NM. Impact of urban morphology on pedestrians: A review of urban approaches. Cities 2022;129:103840. http://dx.doi.org/10.1016/j.cities.2022.103840.
[3] Bongiorno C, Zhou Y, Kryven M, Theurel D, Rizzo A, Santi P, Tenenbaum J, Ratti C. Vector-based pedestrian navigation in cities. Nat Comput Sci 2021;1(10):678–85. http://dx.doi.org/10.1038/s43588-021-00130-y.
[4] Murakami H, Feliciani C, Nishiyama Y, Nishinari K. Mutual anticipation can contribute to self-organization in human crowds. Sci Adv 2021;7(12). http://dx.doi.org/10.1126/sciadv.abe7758.
[5] Mullick P, Fontaine S, Appert-Rolland C, Olivier A-H, Warren WH, Pettré J. Analysis of emergent patterns in crossing flows of pedestrians reveals an invariant of 'stripe' formation in human data. PLoS Comput Biol 2022;18(6):e1010210. http://dx.doi.org/10.1371/journal.pcbi.1010210.
[6] Moussaïd M, Helbing D, Theraulaz G. How simple rules determine pedestrian behavior and crowd disasters. Proc Natl Acad Sci 2011;108(17):6884–8. http://dx.doi.org/10.1073/pnas.1016507108.
[7] Haghani M, Sarvi M. Crowd behaviour and motion: Empirical methods. Transp Res Part B: Methodol 2018;107:253–94. http://dx.doi.org/10.1016/j.trb.2017.06.017.
[8] Duives DC, Daamen W, Hoogendoorn SP. State-of-the-art crowd motion simulation models. Transp Res Part C: Emerg Technol 2013;37:193–209. http://dx.doi.org/10.1016/j.trc.2013.02.005.
[9] Li W, Mahadevan V, Vasconcelos N. Anomaly detection and localization in crowded scenes. IEEE Trans Pattern Anal Mach Intell 2014;36(1):18–32. http://dx.doi.org/10.1109/tpami.2013.111.

[10] Gu H, Kim S, Jung M. Data-driven urban planning for proactive crowd management: Lessons from the 2022 Seoul halloween crowd crush. Cities 2026;168:106418. http://dx.doi.org/10.1016/j.cities.2025.106418.
[11] Nahavandi S, Alizadehsani R, Nahavandi D, Mohamed S, Mohajer N, Rokonuzzaman M, Hossain I. A comprehensive review on autonomous navigation. ACM Comput Surv 2025;57(9):1–67. http://dx.doi.org/10.1145/3727642.
[12] Jayles B, Escobedo R, Pasqua R, Zanon C, Blanchet A, Roy M, Tredan G, Theraulaz G, Sire C. Collective information processing in human phase separation. Phil Trans R Soc B 2020;375(1807):20190801. http://dx.doi.org/10.1098/rstb.2019.0801.
[13] Helbing D, Farkas I, Vicsek T. Simulating dynamical features of escape panic. Nature 2000;407(6803):487–90. http://dx.doi.org/10.1038/35035023.
[14] Wu W, Zheng X. A systematic analysis of subgroup research in pedestrian and evacuation dynamics. IEEE Trans Intell Transp Syst 2024;25(2):1225–46. http://dx.doi.org/10.1109/tits.2023.3318417.
[15] Zhou C, Han M, Liang Q, Hu Y-F, Kuai S-G. A social interaction field model accurately identifies static and dynamic social groupings. Nat Hum Behav 2019;3(8):847–55. http://dx.doi.org/10.1038/s41562-019-0618-2.
[16] Karamouzas I, Skinner B, Guy SJ. Universal power law governing pedestrian interactions. Phys Rev Lett 2014;113(23):238701. http://dx.doi.org/10.1103/physrevlett.113.238701.
[17] Haghani M. Empirical methods in pedestrian, crowd and evacuation dynamics: Part I. experimental methods and emerging topics. Saf Sci 2020;129:104743. http://dx.doi.org/10.1016/j.ssci.2020.104743.
[18] Haghani M. Empirical methods in pedestrian, crowd and evacuation dynamics: Part II. Field methods and controversial topics. Saf Sci 2020;129:104760. http://dx.doi.org/10.1016/j.ssci.2020.104760.
[19] Corbetta A, Meeusen JA, Lee C-m, Benzi R, Toschi F. Physics-based modeling and data representation of pairwise interactions among pedestrians. Phys Rev E 2018;98(6):062310. http://dx.doi.org/10.1103/physreve.98.062310.
[20] Murakami H, Tomaru T, Feliciani C, Nishiyama Y. Spontaneous behavioral coordination between avoiding pedestrians requires mutual anticipation rather than mutual gaze. IScience 2022;25(11):105474. http://dx.doi.org/10.1016/j.isci.2022.105474.
[21] Bacik KA, Sobota G, Bacik BS, Rogers T. Order–disorder transition in multidirectional crowds. Proc Natl Acad Sci 2025;122(14). http://dx.doi.org/10.1073/pnas.2420697122.
[22] Kwon J-H, Kim J, Kim S, Cho G-H. Pedestrians safety perception and crossing behaviors in narrow urban streets: An experimental study using immersive virtual reality technology. Accid Anal Prev 2022;174:106757. http://dx.doi.org/10.1016/j.aap.2022.106757.
[23] Liu W, Zhang J, Li X, Song W. Avoidance behaviors of pedestrians in a virtual-reality-based experiment. Phys A 2022;590:126758. http://dx.doi.org/10.1016/j.physa.2021.126758.
[24] Nicolas A, Hassan FH. Social groups in pedestrian crowds: review of their influence on the dynamics and their modelling. Transp A: Transp Sci 2021;19(1). http://dx.doi.org/10.1080/23249935.2021.1970651.
[25] Wu W, Yi W, Wang X, Zheng X. A force-based model for adaptively controlling the spatial configuration of pedestrian subgroups at non-extreme densities. Transp Res Part C: Emerg Technol 2023;152:104154. http://dx.doi.org/10.1016/j.trc.2023.104154.
[26] Moussaïd M, Perozo N, Garnier S, Helbing D, Theraulaz G. The walking behaviour of pedestrian social groups and its impact on crowd dynamics. PLoS One 2010;5(4):e10047. http://dx.doi.org/10.1371/journal.pone.0010047.
[27] Bruneau J, Olivier A-H, Pettre J. Going through, going around: A study on individual avoidance of groups. IEEE Trans Vis Comput Graphics 2015;21(4):520–8. http://dx.doi.org/10.1109/tvcg.2015.2391862.
[28] Gregorj A, Yücel Z, Zanlungo F, Feliciani C, Kanda T. Social aspects of collision avoidance: a detailed analysis of two-person groups and individual pedestrians. Sci Rep 2023;13(1). http://dx.doi.org/10.1038/s41598-023-32883-z.
[29] Gregorj A, Yücel Z, Zanlungo F, Kanda T. Ecological data reveal imbalances in human–human collision avoidance due to dyads' social interaction. Transp Res Part F: Traffic Psychol Behav 2025;109:1313–33. http://dx.doi.org/10.1016/j.trf.2025.01.039.
[30] Pellegrini S, Ess A, Schindler K, van Gool L. You'll never walk alone: Modeling social behavior for multi-target tracking. In: 2009 IEEE 12th international conference on computer vision. IEEE; 2009, http://dx.doi.org/10.1109/iccv.2009.5459260.
[31] Lerner A, Chrysanthou Y, Lischinski D. Crowds by example. Comput Graph Forum 2007;26(3):655–64. http://dx.doi.org/10.1111/j.1467-8659.2007.01089.x.
[32] Gu X, Li C, Gao L, Niu X. A review of pedestrian trajectory prediction methods based on deep learning technology. Sensors 2025;25(23):7360. http://dx.doi.org/10.3390/s25237360.
[33] Wu W, Yi W, Li J, Chen M, Zheng X. Automatic identification of human subgroups in time-dependent pedestrian flow networks. IEEE Trans Multimed 2024;26:166–77. http://dx.doi.org/10.1109/tmm.2023.3262975.
[34] Tomaru T, Nishiyama Y, Feliciani C, Murakami H. Robust spatial self-organization in crowds of asynchronous pedestrians. J R Soc Interface 2024;21(214). http://dx.doi.org/10.1098/rsif.2024.0112.
[35] Mahan GD. Many-particle physics. Springer US; 2000, http://dx.doi.org/10.1007/978-1-4757-5714-9.
[36] Olivier A-H, Marin A, Crétual A, Pettré J. Minimal predicted distance: A common metric for collision avoidance during pairwise interactions between walkers. Gait Posture 2012;36(3):399–404. http://dx.doi.org/10.1016/j.gaitpost.2012.03.021.
[37] Wu W, Yi W, Wang X, Zheng X. A vision-driven model based on cognitive heuristics for simulating subgroup behaviors during evacuation. IEEE Trans Intell Transp Syst 2024;25(11):16048–58. http://dx.doi.org/10.1109/tits.2024.3421626.
[38] Salazar-Miranda A, Fan Z, Baick M, Hampton KN, Duarte F, Loo BPY, Glaeser E, Ratti C. Exploring the social life of urban spaces through AI. Proc Natl Acad Sci 2025;122(30). http://dx.doi.org/10.1073/pnas.2424662122.
[39] Ge J, Zhang J, Chang C, Zhang Y, Yao D, Li L. Task-driven controllable scenario generation framework based on AOG. IEEE Trans Intell Transp Syst 2024;25(6):6186–99. http://dx.doi.org/10.1109/tits.2023.3347535.
[40] Ge J, Zhang J, Chang C, Zhang Y, Yao D, Tian Y, Li L. Dynamic testing for autonomous vehicles using random quasi Monte Carlo. IEEE Trans Intell Veh 2024;9(3):4480–92. http://dx.doi.org/10.1109/tiv.2024.3358329.
[41] Gallup AC, Hale JJ, Sumpter DJT, Garnier S, Kacelnik A, Krebs JR, Couzin ID. Visual attention and the acquisition of information in human crowds. Proc Natl Acad Sci 2012;109(19):7245–50. http://dx.doi.org/10.1073/pnas.1116141109.
[42] Battiston F, Amico E, Barrat A, Bianconi G, Ferraz de Arruda G, Franceschiello B, Iacopini I, Kéfi S, Latora V, Moreno Y, Murray MM, Peixoto TP, Vaccarino F, Petri G. The physics of higher-order interactions in complex systems. Nat Phys 2021;17(10):1093–8. http://dx.doi.org/10.1038/s41567-021-01371-4.